

# Collision Dynamics of Two Bose-Einstein Condensates in the Presence of Raman Coupling

Tao Hong, Tadao Shimizu

*Department of Electronics and Computer Science, Science University of Tokyo in Yamaguchi,  
1-1-1 Daigaku-dori, Onoda, Yamaguchi 756-0884, Japan.*

## Abstract

A collision of two-component Bose-Einstein condensates in the presence of Raman coupling is proposed and studied by numerical simulations. Raman transitions are found to be able to reduce collision-produced irregular excitations by forming a time-averaged attractive optical potential. Raman transitions also support a kind of dark soliton pairs in two-component Bose-Einstein condensates. Soliton pairs and their remnant single solitons are shown to be controllable by adjusting the initial relative phase between the two colliding condensates or the two-photon detuning of Raman transitions.

PACS Numbers: 03.75.Fi, 32.80.Pj

## I. INTRODUCTION

The realization of high-density Bose-Einstein condensates [1] invokes the study of non-linear dynamics of matter waves and inventions of various optical techniques to manipulate Bose-Einstein condensates as well as constructions of various matter-wave interferometers for precision measurements. Usually, people would like to reduce irregular excitations and preserve the coherent property of high-density Bose-Einstein condensates as well as possible in many manipulating processes. However, due to the interactions between atoms, the strong repulsive interactions between Bose-Einstein condensates often lead to irregular excitations, especially in colliding processes. Inventing a convenient optical technique, which can reduce irregular excitations as well as exert effective controlling on the Bose-Einstein condensates, is very important.

Raman coupling is a very successful experimental technique in manipulating ultra-cold atomic gas between different internal and external states because it has the merit of avoiding spontaneous emission loss of atoms in transition processes. For example, recently several experiments have already successfully employed Raman coupling in manipulating Bose-Einstein condensates [2].

Here by proposing a Raman coupling scheme of atomic Bose-Einstein condensates, we show that Raman coupling can also be used to reduce irregular excitations produced in a colliding process of two Bose-Einstein condensates. Instead of irregular excitations, the Raman coupling produces a new type of coherent textures, namely dark soliton pairs in the colliding process. Additionally, we also find that these dark soliton pairs and their remnant dark solitons are very sensitive to the initial relative phase between Bose-Einstein condensates and the two-photon detuning of Raman transitions.

The paper is organized as follows. In Sec. II, we introduce the proposed colliding process of two Bose-Einstein condensates in the presence of Raman coupling, and the two coupled Gross-Pitaevskii equations for the description of this colliding process. In Sec. III, first we do some simplifications, then we show numerical simulations of the colliding process, analyze

the function of Raman coupling in the colliding process, and discuss the physical origin and some special properties of dark soliton pairs. In Sec. IV, we draw conclusions as well as point out some potential applications of the proposed colliding process.

## II. THEORETICAL MODEL

First, we introduce the proposal in detail by using a schematic diagram in Fig. 1. The black frame, in Fig. 1(a), represents a transverse confining potential  $V_0(x, y)$  for two atomic Bose-Einstein condensates 1 and 2 in the abstract. This potential can be formed, for example, by a blue-detuned hollow laser beam propagating along z-axis, which has already been demonstrated to be very effective in the recent experiment [3]. Additionally, there are two red-detuned Gaussian laser beams 1 and 2 propagating along x-axis. The intensities of two laser beams are uniform in x and y directions, but in Gaussian shape in z direction, as indicated by the gray levels. Their frequencies are  $\omega_1$  and  $\omega_2$  respectively, as shown in Fig. 1(b). As to the condensates, we assume that atoms have three internal states,  $|g_1\rangle$ ,  $|g_2\rangle$  and  $|e\rangle$ . Thus the two laser beams couple them together and form two Rabi transitions respectively, as shown in Fig. 1(b). Because of the negative detuning ( $\Delta < 0$ ) and nonuniform intensities of the two laser beams, they can form two z-axial confining potentials for condensates 1 and 2 respectively, which are assumed to be initially distributed in states  $|g_1\rangle$  and  $|g_2\rangle$  respectively. Additionally, we assume that the laser beams 1 and 2 are initially separated by a distance and moving at velocities  $v_1$  and  $v_2$  respectively in opposite directions. Thus the two condensates are trapped by the two laser beams and moving at velocities same as those of laser beams in opposite directions. While the two laser beams overlap, the condensates in the overlap region are transferred between states  $|g_1\rangle$  and  $|g_2\rangle$  due to the occurrence of Raman transitions. As the two condensates go very close, they collide and interfere with each other.

Next, we derive the equation for the description of this proposal. As shown in Fig. 1(b), because atoms have three internal states, first we generally consider a condensate consist-

ing of three components. To avoid spontaneous emission in Raman-transition process, we assume that the intermediate detuning  $\Delta$  of laser beams 1 and 2 is much larger than other characteristic frequencies, such as the natural line width of the atomic transitions and the two-photon detuning  $\delta$ . As a result, the evolution of the  $|e\rangle$ -state component adiabatically follows the  $|g_1\rangle$  and  $|g_2\rangle$ -state components, i.e.,  $\Psi_e = -(\Omega_1 e^{-i\omega_1 t} \Psi_{g_1} + \Omega_2 e^{-i\omega_2 t} \Psi_{g_2})/(2\Delta)$ , where  $\Psi_e, \Psi_{g_1}$  and  $\Psi_{g_2}$  are the macroscopic wave functions of the three-component Bose-Einstein condensate in states  $|e\rangle$ ,  $|g_1\rangle$  and  $|g_2\rangle$  respectively. Then, at zero temperature and under rotating-wave approximation, the light-coupled  $|g_1\rangle$  and  $|g_2\rangle$ -state components can be described by the following coupled Gross-Pitaevskii equations:

$$i\hbar \frac{\partial \Psi_{g_1}}{\partial t} = -\frac{\hbar^2}{2m} \nabla^2 \Psi_{g_1} + V_0(x, y) \Psi_{g_1} + V_{g_1}(z, t) \Psi_{g_1} + U_0 |\Psi_{g_1}|^2 \Psi_{g_1} + U_0 |\Psi_{g_2}|^2 \Psi_{g_1} + \hbar R(z, t) \Psi_{g_2} \quad (1)$$

$$i\hbar \frac{\partial \Psi_{g_2}}{\partial t} = -\frac{\hbar^2}{2m} \nabla^2 \Psi_{g_2} + \hbar \omega_g \Psi_{g_2} + V_0(x, y) \Psi_{g_2} + V_{g_2}(z, t) \Psi_{g_2} + U_0 |\Psi_{g_2}|^2 \Psi_{g_2} + U_0 |\Psi_{g_1}|^2 \Psi_{g_2} + \hbar R^*(z, t) e^{i(\omega_2 - \omega_1)t} \Psi_{g_1} \quad (2)$$

where  $m$  is the atomic mass.  $U_0$  describes the atomic interaction strength, which is related to the s-wave scattering length  $a_{sc}$  by  $U_0 = 4\pi\hbar^2 a_{sc}/m$ . Here we assume that  $a_{sc} > 0$  and it is same for all collisions between atoms in same or different internal states.  $V_0(x, y)$  denotes the transverse confining potential, which is common for both  $|g_1\rangle$  and  $|g_2\rangle$ -state components.  $V_{g_1}(z, t) = \hbar|\Omega_1(\mathbf{r}, t)|^2/(4\Delta)$  and  $V_{g_2}(z, t) = \hbar|\Omega_2(\mathbf{r}, t)|^2/(4\Delta)$  are two localized optical potentials produced by the laser beams 1 and 2 respectively.  $R(z, t) = \Omega_1^*(\mathbf{r}, t)\Omega_2(\mathbf{r}, t)/(4\Delta)$  is the effective Rabi frequency of two-photon transitions. Because the laser beams 1 and 2 are in Gaussian shape and moving along z-axis, their corresponding Rabi frequencies can be written as  $\Omega_1(\mathbf{r}, t) = \Omega_{10} e^{-(z-z_{01}-v_1 t)^2/a_1^2} e^{-i\mathbf{k}_1 \cdot \mathbf{r}}$  and  $\Omega_2(\mathbf{r}, t) = \Omega_{20} e^{-(z-z_{02}-v_2 t)^2/a_2^2} e^{-i\mathbf{k}_2 \cdot \mathbf{r}}$ , where  $\Omega_{10}$  and  $\Omega_{20}$  are maximum magnitudes of the two Rabi frequencies,  $z_{01}$  and  $z_{02}$  are initial center positions,  $a_1$  and  $a_2$  are half widths, and  $\mathbf{k}_1$  and  $\mathbf{k}_2$  are wave vectors of the two laser beams respectively. Additionally, we assume that the wave vectors  $\mathbf{k}_1$  and  $\mathbf{k}_2$  are approximately equal, then the two-photon Rabi frequency can be written as

$R(z, t) = \Omega_{10}\Omega_{20}e^{-(z-z_{01}-v_1t)^2/a_1^2-(z-z_{02}-v_2t)^2/a_2^2}/(4\Delta)$ . It is evident that when and only when the two potentials,  $V_{g1}(z, t)$  and  $V_{g2}(z, t)$ , overlap with each other, the effective two-photon Rabi frequency becomes finite. All together, we reduce the description of the Bose-Einstein condensate from three components to two components now.

### III. NUMERICAL SIMULATION

For simplicity and to give more prominence to the analysis of the affection of Raman transitions on the collision, we need to do some simplifications. We assume the transverse confining potential  $V_0(x, y)$  is so tight and the z-axial confining potentials,  $V_{g1}(z, t)$  and  $V_{g2}(z, t)$ , are so loose: that in the description of the transverse modes of the Bose-Einstein condensate, we can neglect the affection of  $V_{g1}(z, t)$  and  $V_{g2}(z, t)$  as well as interactions between atoms; that in the description of the longitudinal modes, we can find that the longitudinal dimension of the condensate is much larger than the healing length. We can also find that the transverse dimensions of the condensate are very small, and the time scale for adjustment of the transverse profile of the condensate to the equilibrium form appropriate for the instantaneous number of atoms per unit length is small compared with the time for an excited pulse to pass a given point. This is a low-density approximation, in fact, similar to that used in Ref. [4]. Thus by letting  $\Psi_{g1}(\mathbf{r}, t) = f_{g1}(z, t)g_{g1}(x, y)e^{-i\mu_1t/\hbar}$  and  $\Psi_{g2}(\mathbf{r}, t) = f_{g2}(z, t)g_{g2}(x, y)e^{-i\mu_2t/\hbar}$  and through a deduction similar to that in Ref. [4], we can get simplified one-dimensional Gross-Pitaevskii equations,

$$i\hbar\frac{\partial f_{g1}}{\partial t} = -\frac{\hbar^2}{2m}\frac{\partial^2 f_{g1}}{\partial z^2} + V_{g1}(z, t)f_{g1} + U'_0|f_{g1}|^2f_{g1} + U''_0|f_{g2}|^2f_{g1} + \hbar R(z, t)e^{-i(\mu_2-\mu_1)t/\hbar}f_{g2} \quad (3)$$

$$i\hbar\frac{\partial f_{g2}}{\partial t} = -\frac{\hbar^2}{2m}\frac{\partial^2 f_{g2}}{\partial z^2} + \hbar\omega_g f_{g2} + V_{g2}(z, t)f_{g2} + U'_0|f_{g2}|^2f_{g2} + U''_0|f_{g1}|^2f_{g2} + \hbar R^*(z, t)e^{i(\omega_2-\omega_1)t+i(\mu_2-\mu_1)t/\hbar}f_{g1} \quad (4)$$

where  $g_{g1}$  and  $g_{g2}$  are the normalized transverse modes of the two components,  $\mu_1$  and  $\mu_2$  are the chemical potentials of  $g_{g1}$  and  $g_{g2}$  respectively,  $f_{g1}$  and  $f_{g2}$  are the longitudinal wave functions,  $U'_0 = U_0 \int |g_{g1}(x, y)|^4 dx dy$  and  $U''_0 = U_0 \int |g_{g1}(x, y)g_{g2}(x, y)|^2 dx dy$ .

As an initial condition for the colliding process, we assume that the two-component Bose-Einstein condensate is initially separated into two condensates, i.e.,  $\Psi_{g1}(\mathbf{r}, t)|_{t=0}$  and  $\Psi_{g2}(\mathbf{r}, t)|_{t=0}$ , which are trapped in the ground states of the two moving potentials,  $V_{g1}(z, t)$  and  $V_{g2}(z, t)$ , respectively. For simplicity, we assume that the two potentials have same shapes, depths and speeds (but in opposite directions), thus the transverse and longitudinal modes of the two initial ground-state Bose-Einstein condensates are in same shape and the condensates has same numbers of atoms and same chemical potentials.

Then we use split operator method to solve the above time dependent Gross-Pitaevskii Eqs.3 and 4. First, we show a typical colliding process in the presence of Raman coupling in Figs. 2(a), (b) and Fig. 3. For comparison, in Figs. 2(c) and (d), we also show another different collision in which two condensates same as the above are trapped by two potentials similar to  $V_{g1}(z, t)$  and  $V_{g2}(z, t)$ , but there are no Raman transitions between them. The elimination of Raman transitions is possible so long as the two laser beams couple the two ground states  $|g_1\rangle$  and  $|g_2\rangle$  with different excited states respectively instead of one common excited state. The parameter values used in the numerical simulation are as following:  $\Omega_{10}^2/(4\Delta) = \Omega_{20}^2/(4\Delta) = \Omega_{10}\Omega_{20}/(4\Delta) = -6000/\tau$ ,  $v_1 = -v_2 = 9a_1/\tau$ ,  $a_2 = a_1$ ,  $U'_0 = U''_0 = 2000\hbar/\tau$ ,  $z_{01} = -z_{02} = -a_1$ , and the chemical potentials of initial ground-state Bose-Einstein condensates are both  $\mu_0 = -3.99 \times 10^3\hbar/\tau$ , where  $a_1$  and  $\tau = 2ma_1^2/\hbar$  are considered as the unit length and the unit time respectively.

In the collision without Raman transitions, the two condensates obstruct their passing through each other because of repulsive interactions between atoms, as shown in Figs. 2(c) and (d). After the collision, we can see that small parts of condensates radiate out of the axial optical potentials, the remnant Bose-Einstein condensates oscillate violently in the potentials. The violent oscillations appear to be very irregular. In contrast, Figs. 2(a), (b) and Fig. 3 show that while Raman transitions exist, the radiations become very weak, the violent oscillations of remnant Bose-Einstein condensates are much reduced. This indicates that the repulsive interaction between two Bose-Einstein condensates is greatly counteracted by an attractive optical potential produced by Raman transitions. We can understand

the formation of this potential in this way. Because Raman transitions can transfer each condensate between two components,  $f_{g1}$  and  $f_{g2}$  circularly, each condensate interacts with the two axial optical potentials  $V_{g1}$  and  $V_{g2}$  alternatively. As a result, the light-shifted energy of each condensate, produced by the two laser beams, becomes a temporal combination of  $V_{g1}$  and  $V_{g2}$ , and each condensate feels a vibrating optical potential locating at the collision center  $z = 0$ . According to the overlap form of  $V_{g1}$  and  $V_{g2}$ , the vibrating potential, in average, is attractive. Thus this time-averaged attractive potential counteracts the repulsive interaction between two condensates, so it becomes much easier for them to pass through each other. We therefore observe the oscillation amplitudes of condensates, produced by the repulsive interaction, become much small. But between  $t = 0.05\tau$  and  $0.15\tau$ , we can still observe that the volume of each condensate oscillates slightly in the colliding process due to the vibration of the attractive optical potential.

In the colliding process, we also observe that dark solitons are generated, as shown in Fig. 3. Formations of dark solitons are due to the interference of colliding condensates. Although the two condensates are initially distributed in two different internal states respectively, Raman transitions can transfer parts of them from one of the internal states to the other in the colliding process. Consequently, when the transferred part of one condensate overlaps with the part of the other condensate in the same internal state, interference fringes are produced. Due to nonlinear effect of condensates, interference fringes evolve into dark solitons. It is evident that this process is similar to that in Ref. [6].

However, solitons produced in this colliding process in the presence of Raman coupling are quite different from those single solitons described in Ref. [4,5,8]. One of important differences is that these solitons always appear in pairs. As shown in Figs. 3(a)-(d), in the colliding process, every soliton in one component of the condensates always has a corresponding soliton in the other component at the same spatial position. Another important difference is that the density difference between two components does not lead to a speed difference between two solitons in a pair. As shown in Figs. 3(a) and (b), sometimes the two components have quite different local densities at the location of a soliton pair, how-

ever, solitons in the pair always move synchronously in the condensates. The reason for synchronous motion of two solitons in a pair is that Raman transitions associate the two components tightly and consequently locks their phases together. As we can see in Fig. 4, the phases of two components are almost completely same in the region of strong Raman transitions that are indicated by magnitudes of the normalized two-photon Rabi frequency  $|4R\Delta/(\Omega_{10}\Omega_{20})|$ . Dark solitons are phase kinks in essence, so there is no doubt that solitons, with similar spatial phases, in a pair move synchronously. Additionally, the cross phase modulation between dark solitons in a pair also makes a repulsive effect between them, and tends to separate them. It is evident that this repulsive effect is also counteracted by Raman transitions, which produce an equivalently attractive effect between solitons in the pair by locking their phases together. Even after a collision of two soliton pairs A and B, solitons in each pair can still preserve their waveforms and trajectories well, as shown in Figs. 3(b)-(c) and Figs. 2(a)-(b) respectively. This illustrates that collisions between soliton pairs are elastic collisions, which are usually considered as an important common characteristic of all kinds of solitons. The synchronous motion of solitons in the pair also indicates the propagation speed of the soliton pair is determined by the total local density of the two components instead of each one component. We can find this property from Figs. 2(a)-(b). The propagation speed of the soliton pair, in the region  $z < 0$ , at time  $t = 0.078\tau$  is larger than that at time  $t = 0.047\tau$ , because the total density of the two components is increased in the overlap region,. Some similarities between a soliton pair and a single soliton can also be seen. For example, the propagation speed, the width and the density contrast of a soliton pair also depend on the value of its phase kink that is also varied by the local density gradient. We can find these properties by a careful observation of Figs. 2(a)-(b), Fig. 3 and Fig. 4. Because the density of the condensates varies in parabola-like form in space, we can find its phase kink flips in the boundary region of the condensates, simultaneously its speed flips too, and as a result, the soliton pair oscillates inside the condensates.

The two components of the condensates begin to separate very apparently after  $t = 0.15\tau$ , because of the separation of the two axial optical potentials, as shown in Figs. 2(a)-(b).

Simultaneously, Raman transitions become weaker and weaker because of the decrement of the overlap of the two laser beams, as shown in Figs. 3(d)-(f). As a result, soliton pairs become unstable and are to be separated in this process. Critically depending on the local evolution of the two components, some solitons disappear and some of them remain and propagate into the separated one-component condensates, as shown in Figs. 2(a)-(b) and Figs. 3(e)-(f). Because of the disappearance of cross phase modulation in each one-component condensate, the oscillation behaviors of remnant single solitons are different from those of soliton pairs. Especially, the oscillation periods of remnant single solitons appear to be quite different from those of previous soliton pairs.

The generation of dark soliton pairs is controllable. Usually, the relative phase between two condensates in different internal states is meaningless because of the orthogonality of the internal states. However, here Raman transitions can form a circulation of atoms between the two internal states, the relative phase between the two condensates are related and therefore becomes very important. Because the formation of dark soliton pairs is due to the interference of colliding condensates, we can also control the generation of soliton pairs as well as remnant single solitons by adjusting the initial relative phase between two colliding condensates or the two-photon detuning of Raman transitions, as shown in Fig. 5.

In the above, we have discussed the collision of two Bose-Einstein condensates under the one-dimensional approximation, then will a three dimensional collision be completely different from the one-dimensional collision? Some difference must exist. For example, in three-dimensional process, dark soliton pairs might be distorted by transverse perturbations and evolve into vortices because similar behaviors of single dark solitons have been found [8]. However, in the above analysis, we have already found that the function of Raman coupling in the colliding process is, in fact, to lock the phases of the two components of the condensates by forming the strong atom circulation between the two internal states, and as a result, solitons appear in pairs. As for vortices, they are phase singular points, so they are quit similar to dark solitons in essence. We think that Raman coupling can also lock the phases of two components of the condensates in a three-dimensional case, and vortex

pairs might therefore be formed. Certainly, more affirmative answer should be gotten in a numerical simulation of a three-dimensional collision, which will be done in the future work.

#### IV. CONCLUSION

In conclusion, we have proposed a new Raman coupling scheme of Bose-Einstein condensates, and analyzed the influence of Raman transitions on the collision and excitation of two-component Bose-Einstein condensates. We have found that Raman transitions can reduce collision-produced irregular excitations by forming a time-averaged attractive potential. Raman transitions also support a new kind of dark solitons, i.e., dark soliton pairs in two-component Bose-Einstein condensates, by locking the phases of the two components. We have also shown the control of soliton pairs and their remnant single solitons by adjusting the initial relative phase between the two colliding condensates and the two-photon detuning of Raman transitions. The dynamical sensitivity of the dark soliton pairs and remnant solitons to these parameters indicates that the proposed collision can be used in the measurement of relative phase between different high-density Bose-Einstein condensates. Currently, people are considering constructions of various interferometers with matter waves for high precision measurements. We think that this proposal might provide a useful method to this area.

#### ACKNOWLEDGMENTS

T. Hong thanks Japan Science Promotion Society for the partial financial support. This work is supported by a Grant-in-Aid for JSPS Fellows from the Ministry of Education, Science, Sports and Culture of Japan.

## REFERENCES

- [1] M. H. Anderson, J. R. Ensher, M. R. Matthews, C. E. Wieman, and E. A. Cornell, *Science* **269**, 198 (1995); K. Davis, M.-O. Mewes, M. R. Andrews, N. J. van Druten, D. S. Durfee, D. M. Kurn, and W. Ketterle, *Phys. Rev. Lett.* **75**, 3969 (1995); C. C. Bradley, C. A. Sackett, J. J. Tollet, and R. G. Hulet, *Phys. Rev. Lett.* **78**, 985 (1997); D. G. Fried, T. C. Killian, L. Willmann, D. Landhuis, S. C. Moss, D. Kleppner, and T. J. Greytak, *Phys. Rev. Lett.* **81**, 3811 (1998).
- [2] E. W. Hagley, L. Deng, M. Kozuma, J. Wen, K. Helmerson, S. L. Rolston, W. D. Phillips, *Science* **283**, 1706 (1999); M.-O. Mewes et al., *Phys. Rev. Lett.* **78**, 582 (1997); I. Bloch, T. W. Hänsch, and T. Esslinger, *Phys. Rev. Lett.* **82**, 3008 (1998); B. P. Anderson and M. A. Kasevich, *Science* **282**, 1686 (1998); A. P. Chikkatur, A. Görlitz, D. M. Stamper-Kurn, S. Inouye, S. Gupta, and W. Ketterle, *Phys. Rev. Lett.*, **85**, 483 (2000).
- [3] K. Bongs, S. Burger, S. Dettmer, D. Hellweg, J. Arlt, W. Ertmer, and K. Sengstock, e-print cond-mat/0007381.
- [4] A. D. Jackson et al., *Phys. Rev. A* **58**, 2417 (1998).
- [5] W. Zhang et al., *Phys. Rev. Lett.* **72**, 60 (1994); W. P. Reinhardt and C. W. Clark, *J. Phys. B* **30**, L785 (1997); T. Hong et al., *Phys. Rev. A*, **58**, 3128 (1998); A. E. Muryshev et al., *Phys. Rev. A* **60**, R2665 (1999); P. O. Fedichev et al., *Phys. Rev. A* **60**, 3220 (1999); Th. Busch and J. R. Anglin, *Phys. Rev. Lett.* **84**, 2298 (2000); L. D. Carr, C. W. Clark, and W. P. Reinhardt, *Phys. Rev. A* **62**, 063610 (2000).
- [6] T. F. Scott et al., *J. Phys. B* **31**, L329 (1998).
- [7] R. Dum, A. Sanpera, K.-A. Suominen, M. Brewczyk, M. Kuś, K. Rzążewski, and M. Lewenstein, *Phys. Rev. Lett.*, **80**, 3899 (1998); B. Jackson, J. F. McCann, and C. S. Adams, *Phys. Rev. Lett.*, **80**, 3903 (1998).
- [8] M. R. Andrews et al., *Phys. Rev. Lett.*, **79**, 553 (1997); S. Burger et al., *Phys. Rev. Lett.*,

**83**, 5198 (1999); J. Denschlag et al., Science, **287**, 97 (2000).

## FIGURES

FIG. 1. (a) Collision and Raman coupling scheme of two atomic Bose-Einstein condensates. (b) Atomic internal energy levels of Bose-Einstein condensates and light coupling.  $|g_1\rangle$ ,  $|g_2\rangle$  denote two ground states and  $|e\rangle$  denotes an excited state, energy eigen values of which are 0,  $\hbar\omega_g$  and  $\hbar\omega_e$  respectively. The laser beams 1 and 2, with frequencies  $\omega_1$  and  $\omega_2$  respectively, couple these states together, forming so-called “ $\Lambda$ ” configuration Raman transitions.  $\Omega_1$  and  $\Omega_2$  are corresponding single-photon Rabi frequencies. The intermediate detuning and two-photon detuning of Raman transitions are  $\Delta = \omega_1 - \omega_e$  and  $\delta = \omega_1 - \omega_2 - \omega_g$  respectively. Direct transitions between  $|g_1\rangle$  and  $|g_2\rangle$  are electric-dipole forbidden.

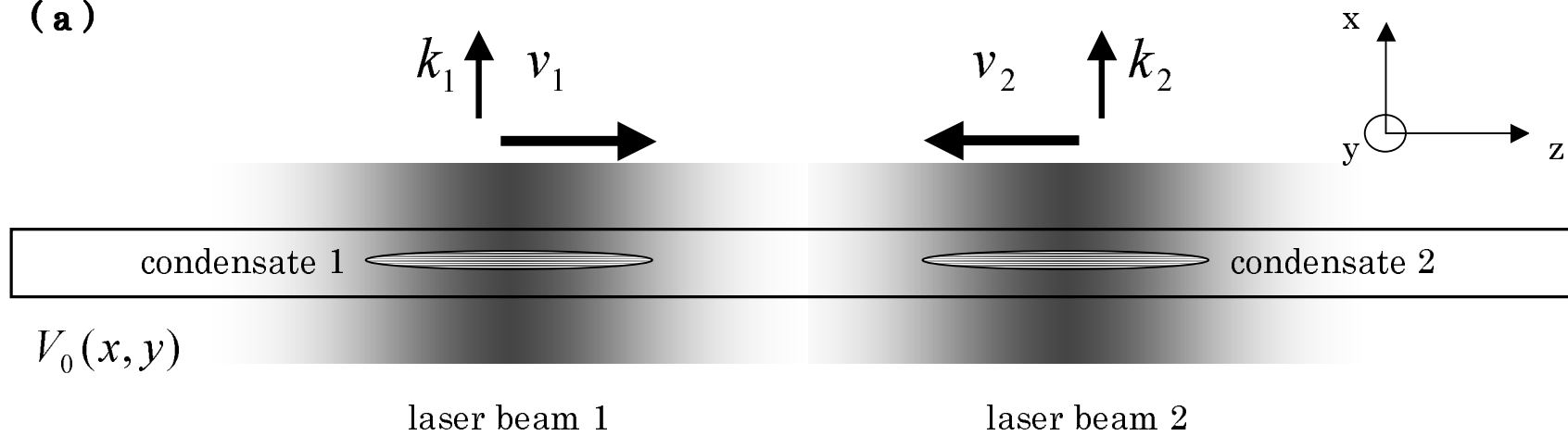
FIG. 2. Contour plots of time evolution of the condensate wave functions  $|f_{g1}|$  and  $|f_{g2}|$  in two colliding processes. (a) is for  $|f_{g1}|$  and (b) is for  $|f_{g2}|$  in the collision with Raman coupling. (c) is for  $|f_{g1}|$  and (d) is for  $|f_{g2}|$  in the collision without Raman coupling. In these collisions, the initial phases of  $f_{g1}$  and  $f_{g2}$  are  $\pi/4$  and 0 respectively, and the detuning  $\delta = 0$ . The dash-dot lines denote the boundaries of the corresponding axial optical potential,  $V_{g1}(z, t)$  or  $V_{g2}(z, t)$ . These boundaries correspond to the boundaries of Gaussian laser beams at the  $1/e$  of maximum intensities. Between  $t = 0.05\tau$  and  $0.15\tau$ , there are four zigzag density dip traces in (a) and (b). These four density dip traces indicate the oscillations of four dark solitons inside the condensates.

FIG. 3. Generation of dark soliton pairs in the collision with Raman coupling and remnant single solitons. The thin solid lines denote  $|f_{g1}/f_0|$ , the thick solid lines denote  $|f_{g2}/f_0|$ , and the dashed lines denote  $|4R\Delta/(\Omega_{10}\Omega_{20})|$ .  $f_0$  is the maximum of  $|f_{g1}|_{t=0}$  and  $|f_{g2}|_{t=0}$ . There are four dark solitons in each figure of (a), (b) and (c). The arrow A marks one soliton pair, and the arrow B marks another soliton pair respectively. The values of  $t$  denote the time of subfigures sampled from the colliding process shown in Fig.2(a) and (b).

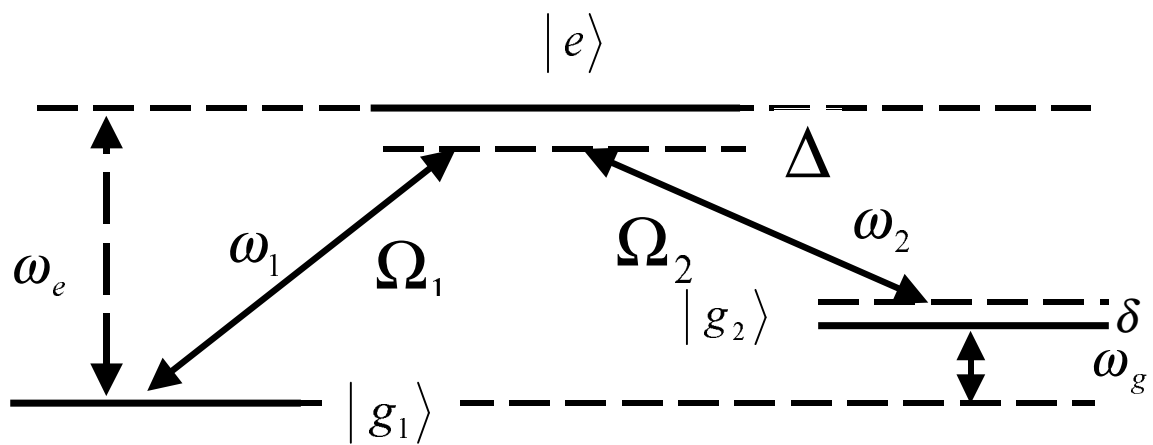
FIG. 4. Phase evolution of the condensate wave functions in the collision with Raman coupling. The solid lines in (a)-(c) denote phase of  $f_{g1}$ , the solid lines in (d)-(f) denote phase of  $f_{g2}/f_{g1}$ , and the dashed lines denote  $|4R\Delta/(\Omega_{10}\Omega_{20})|$ . The arrow A marks the position of one soliton pair, and the arrow B marks the position of the other dark soliton pair respectively. The values of  $t$  denote the time of subfigures sampled from the colliding process shown in Fig.2(a) and (b).

FIG. 5. Contour plots of time evolution of the condensate wave functions  $|f_{g1}|$  and  $|f_{g2}|$  in two colliding processes. (a) is for  $|f_{g1}|$  and (b) is for  $|f_{g2}|$  in one collision. In this collision, the initial phases of  $f_{g1}$  and  $f_{g2}$  are  $\pi/2$  and 0 respectively, and the detuning  $\delta = 0$ . (c) is for  $|f_{g1}|$  and (d) is for  $|f_{g2}|$  in the other collision. In this collision, the initial phases of both  $f_{g1}$  and  $f_{g2}$  are 0s, and the detuning  $\delta = 100/\tau$ . The dash-dot lines denote the boundaries of the corresponding axial optical potential,  $V_{g1}(z, t)$  or  $V_{g2}(z, t)$ . These boundaries correspond to the boundaries of Gaussian laser beams at the  $1/e$  of maximum intensities.

**(a)**

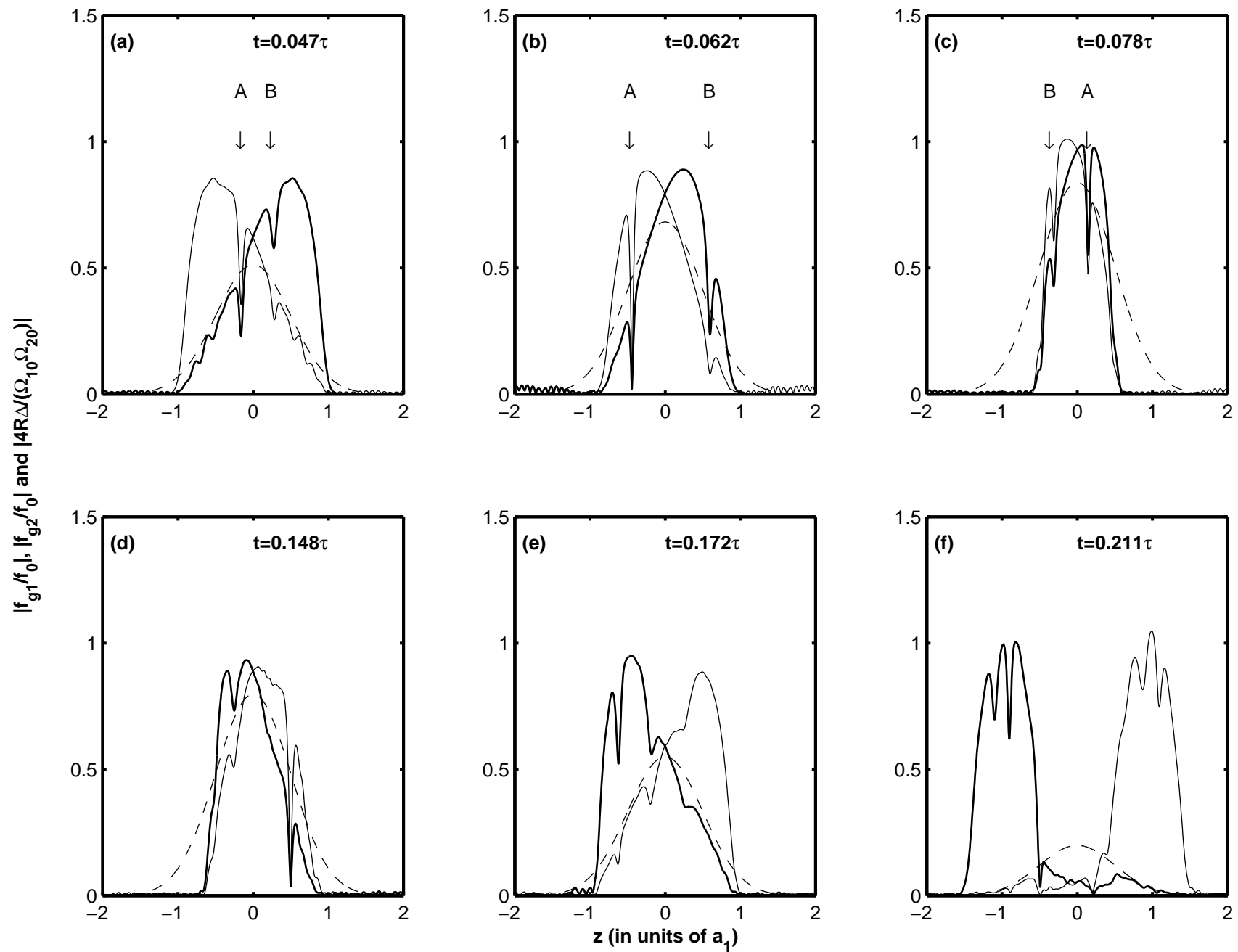


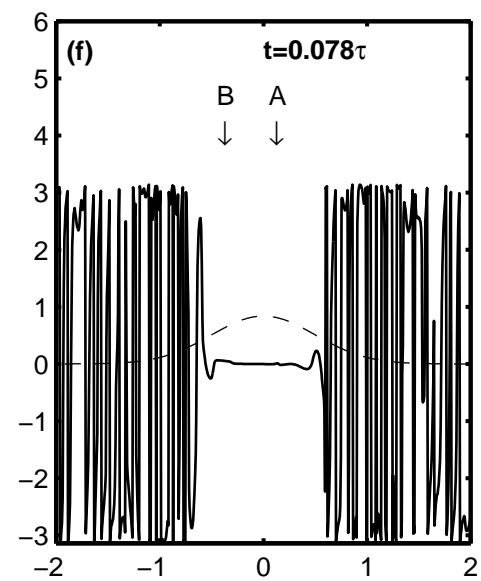
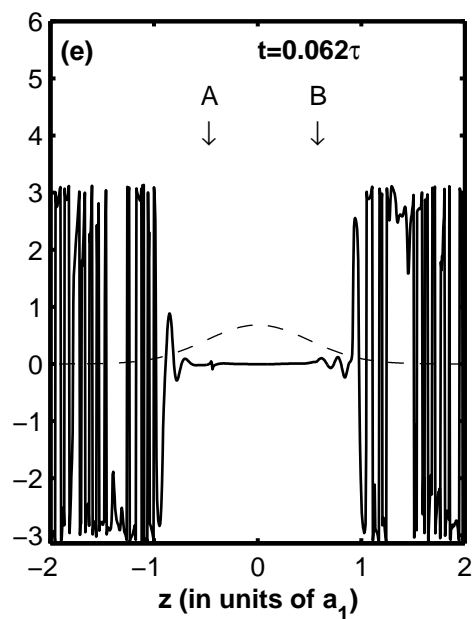
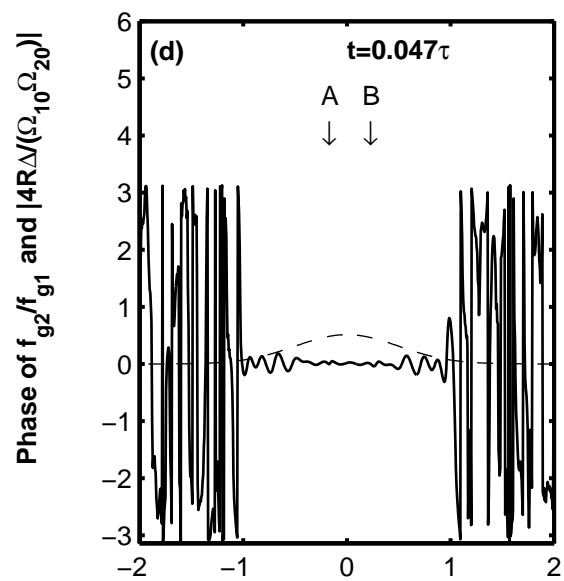
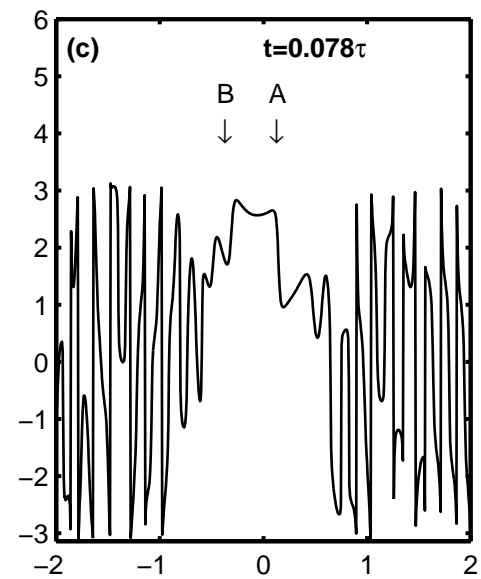
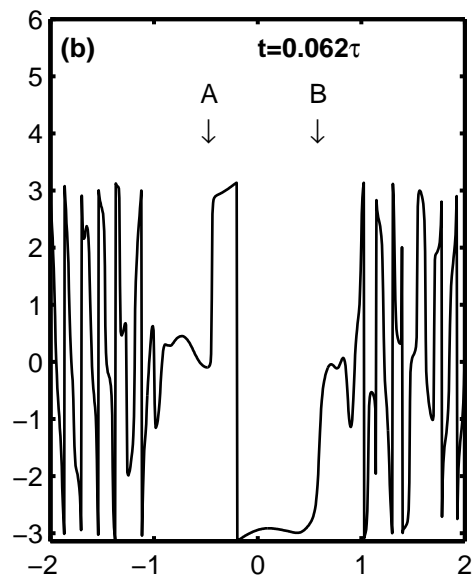
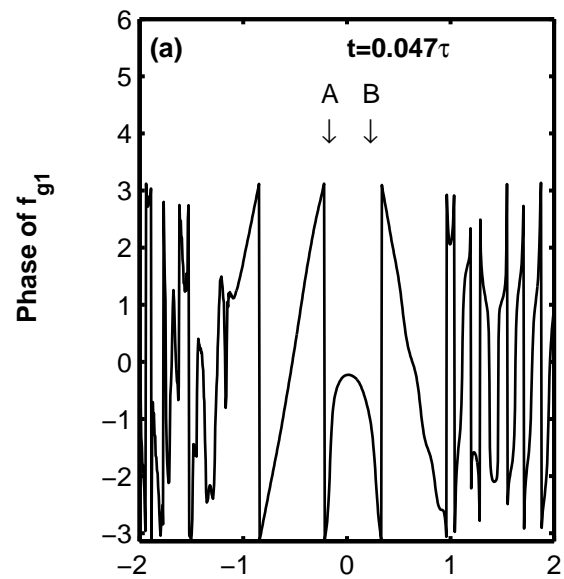
**(b)**



This figure "fig2.jpeg" is available in "jpeg" format from:

<http://arxiv.org/ps/cond-mat/0102004v1>





This figure "fig5.jpeg" is available in "jpeg" format from:

<http://arxiv.org/ps/cond-mat/0102004v1>